Erratum 14 February 2020. See Erratum.

ORGANOMETALLICS

Fluorination of arylboronic esters enabled by bismuth redox catalysis

Oriol Planas*, Feng Wang*, Markus Leutzsch, Josep Cornella†

Bismuth catalysis has traditionally relied on the Lewis acidic properties of the element in a fixed oxidation state. In this paper, we report a series of bismuth complexes that can undergo oxidative addition, reductive elimination, and transmetallation in a manner akin to transition metals. Rational ligand optimization featuring a sulfoximine moiety produced an active catalyst for the fluorination of aryl boronic esters through a bismuth (III)/bismuth (V) redox cycle. Crystallographic characterization of the different bismuth species involved, together with a mechanistic investigation of the carbon-fluorine bond-forming event, identified the crucial features that were combined to implement the full catalytic cycle.

Homogeneous transition-metal catalysis has revolutionized organic synthesis, enabling fast and direct construction of complex functionality. These reactions rely, in large part, on the capacity of noble metals to cycle easily between different oxidation states (Fig. 1A) (*1*). With the goal of providing more sustainable strategies in catalysis, efforts have shifted to unveil the reactivity of more Earth-abundant, first-row transition metals (Fe, Ni, Co, Cu, Mn, and Cr) (*2*–*4*). Chemists have also sought to discover and exploit transition-metal–like reactivity among elements beyond the d-block (*5*–*7*). The concept of the frustrated Lewis pair (FLP) can be applied to boron and phosphorus cooperatively to promote transformations traditionally restricted to transition metals (*8*). Furthermore, methodologies based on alkali (*9*, *10*), alkaline earth (*11*), and group 13 to 17 elements are emerging as acceptable alternatives in certain domains of catalysis (*12*–*16*). These strategies represent useful platforms for chemical synthesis. However, the exploitation of the redox properties of main-group elements in catalysis to access new modes of reactivity is still in its infancy (*17*) and remains a major challenge in organometallic and organic chemistry. We therefore focused our attention on bismuth (Bi), an Earth-abundant and inexpensive main-group element (*18*) with under-explored redox properties (*19*). The use of Bi in catalysis has relied largely on its Lewis acidic properties (*20*), where recent interest has revitalized its use in fields such as C–H activation (*21*), carbonylation (*22*), transfer hydrogenation (*23*), and as the initiator in radical processes (*24*–*26*). We sought to prepare a Bi complex capable of mimicking the canonical, fundamental steps in a transition-metal catalytic cycle: transmetallation (TM), oxidative addition (OA), and reductive elimination (RE) (Fig. 1B). To this end, we focused on the oxidative fluorination of aromatic boronic acids, a transformation that is highly coveted in the pharmaceutical and agrochemical industries (*27*). This reaction is feasible using stoichiometric transition metals, such as Cu (*28*–*30*), Pd (*31*), and Ag (*32*), or hypervalent iodine compounds (*33*). The sole catalytic variant makes use of trifluoroborate aryl salts as substrates, which are converted to aryl fluorides through single-electron transfer processes catalyzed by Pd (*34*). On the basis of the accessibility to Bi compounds in different oxidation states (*35*), we report that the rationally designed bismine complex (**I**) catalyzes fluorination of aryl boronic esters through a Bi(III)/Bi(V) redox cycle.

We hypothesized that a rationally designed ligand would be crucial to exploit the Bi(III)/Bi(V) redox couple. Building on precedents in Bi coordination chemistry (*36*), we sought to take advantage of Bi's capacity for accommodating additional neutral ligands in its coordination sphere, thereby affecting the geometry and the electronics of the Bi center (*37*). Accordingly, we chose a tethered bis-anionic aryl ligand, featuring a linking sulfonyl group in the backbone (Fig. 2A). We predicted that the use of a tether ligand would become important for controlling the geometry in subsequent high-valent intermediates in the catalytic cycle, as Bi(V) compounds are known to undergo dynamic processes such as Berry pseudo-rotation or turnstile rotation (*38*). On the basis of ligand design approaches for high-valent transition metals (*39*), we hypothesized that the lone pair of the S-bound oxygen would become a weak ligand for the Bi center, providing stabilization of putative Bi(V) intermediates. The electron-withdrawing nature of the sulfone group at the ortho position is also expected to render the Bi center more electrophilic, thereby prone to transmetallation and reductive elimination. Additionally, binding two of the three anionic

Max-Planck-Institut für Kohlenforschung, Kaiser-Wilhelm-Platz 1, 45470, Mülheim an der Ruhr, Germany.
*These authors contributed equally to this work.
†Corresponding author. Email: cornella@kofo.mpg.de

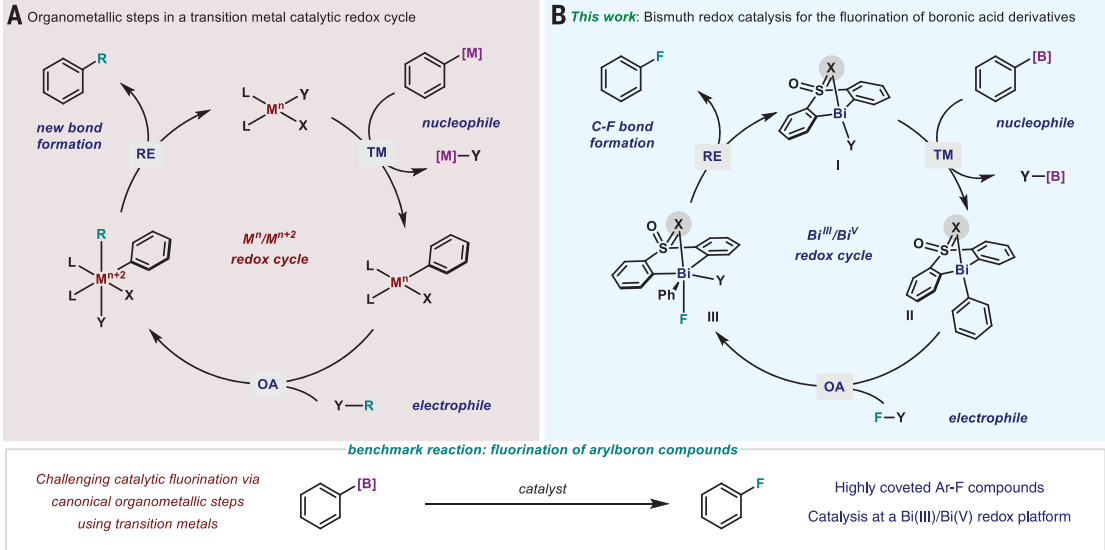

Fig. 1. Can Bi mimic transition-metal behavior in electrophilic fluorination? (**A**) General catalytic two-electron redox cycle of a transition metal. (**B**) Development of an electrophilic fluorination of boronic acid derivatives through a catalytic Bi redox process. L, ligand; M, metal; n, oxidation number; R, organic residue; X, halogen atom (A) or non-anionic ligand (B); Y, anionic ligand.

ligands in a cyclic framework would favor selective reactivity of the unrestrained phenyl group.

With these considerations in mind, we synthesized bismine (**1**) and attempted its oxidation to Bi(V) from the $6s^2$ orbital, through reaction with XeF_2. A smooth conversion to high-valent Bi(V) species was achieved (>95% yield), and x-ray crystallographic analysis revealed a symmetric Bi(V) dimeric structure (**2**) (Fig. 2A). Each Bi atom in **2** adopts a distorted octahedral geometry, with two fluorine atoms positioned trans to each other [F1–Bi1–F2 and F3–Bi2–F4, 164.2(2)°], one of them bridging to the other metal center. The bridging Bi–F bonds are 0.47 Å longer than the terminal bonds. Moreover, the O atoms of the sulfone moiety interact with the Bi centers [Bi1–O1 and Bi2–O2, 3.430(6) Å], thereby forcing the F atom away from linearity and engaging in binding with another Bi, forming a dimer in the solid state. When **2** was heated to 110°C in $CDCl_3$, an unexpected 45% yield of fluorobenzene (**3**) was obtained. This reductive elimination of C–F bond stands in stark contrast to previous reports, in which attempts to thermally induce C–F bond formation from Bi(V) fluoride compounds resulted in decomposition or traces of fluorinated arenes (*40*, *41*). On the basis of the crystallographic information, we anticipated that tuning the electronic properties of the sulfone could influence the Bi(V) center, thus affecting the C–F bond-formation step. Indeed, with a NMe (Me, methyl) group in place of one of the O atoms in the sulfone group (**4**), a notable reduction in yield was observed (**3**, 28%, Fig. 2B). However, when the methyl group in **4** was replaced with CF_3 (**5**), a 94% yield of fluorobenzene (**3**) was obtained after thermal decomposition of the corresponding Bi(V) intermediate. Both **4** and **5** were characterized by x-ray crystallography (Fig. 2B). Despite their comparable Bi–N distances [3.055(2) Å in **4** and 3.038(3) Å in **5**], the electronic nature of the CF_3 group clearly has a notable promotional effect on the reductive elimination process. The elimination of fluorobenzene (**3**) was accompanied by the smooth formation of the corresponding fluorobismine (**6**), which was confirmed by x-ray crystallography. At this point, we presumed that the productive elimination of fluorobenzene from **5** could be ascribed to the low propensity of the NCF_3 group to coordinate to Bi after oxidation, which results in a monomeric Bi(V) difluoride complex. Although attempts to crystallize Bi(V) difluoride compounds derived from **4** and **5** were unsuccessful, the installation of a methyl residue at the ortho position, with respect to the Bi center (**7**), permitted the crystallization of difluorobismine (**8**) (Fig. 2C). X-ray analysis of **8** revealed a monomeric pentavalent complex with trigonal bipyramid geometry (TBP), in which both F atoms occupy apical positions. This geometry is in agreement with the polarity rule for TBP complexes, which predicts that the most electronegative and least sterically demanding substituents are always placed in apical positions—in this case, the fluorides (*42*). As anticipated, coordination of the pending group in **8** is weaker [Bi–N 3.566(4) Å] than in the dimeric sulfone counterpart **2** [Bi–O 3.430(6) Å].

We then turned our attention to the mechanism of this unusual C–F bond reductive elimination. Several para-substituted arylbismine complexes were synthesized (**5** and **9** to **13**, Fig. 3A) and oxidized with XeF_2 to the corresponding pentavalent bismine species (**14** to **19**, Fig. 3A). Thermal decomposition of **14** at 90°C exhibited a first-order kinetic profile (k_{obs} = 1.3 × 10^{-4} s^{-1}, where k_{obs} is the apparent reaction rate constant), in which fluorobenzene (**3**) was produced at the same rate as fluorobismine (**6**) (k_{obs} = 1.0 × 10^{-4} s^{-1} and k_{obs} = 1.1 × 10^{-4} s^{-1}, respectively), reaching 94% yield after 7 hours (Fig. 3A1). An Eyring analysis over a 25°C range revealed a small enthalpy barrier ($\Delta H^{\ddagger}$ = 15.5 ± 0.7 kcal mol^{-1}, where $\Delta H^{\ddagger}$ is the change in enthalpy between reactants and transition state) but a surprisingly high entropic contribution [$\Delta S^{\ddagger}$ = −34.7 ± 1.9 entropy unit (1 e.u. = 1 cal K_{-1} mol_{-1}), where $\Delta S^{\ddagger}$ is the change in entropy between reactants and transition state]. A large and negative value of the entropy parameter is consistent with an associative process in the transition state, although cationic pathways with high degrees of solvent reorganization have also been postulated (*43*, *44*). Hammett kinetic analysis of the thermal decomposition of **14** to **19** to aryl fluorides (**3** and **20** to **24**)

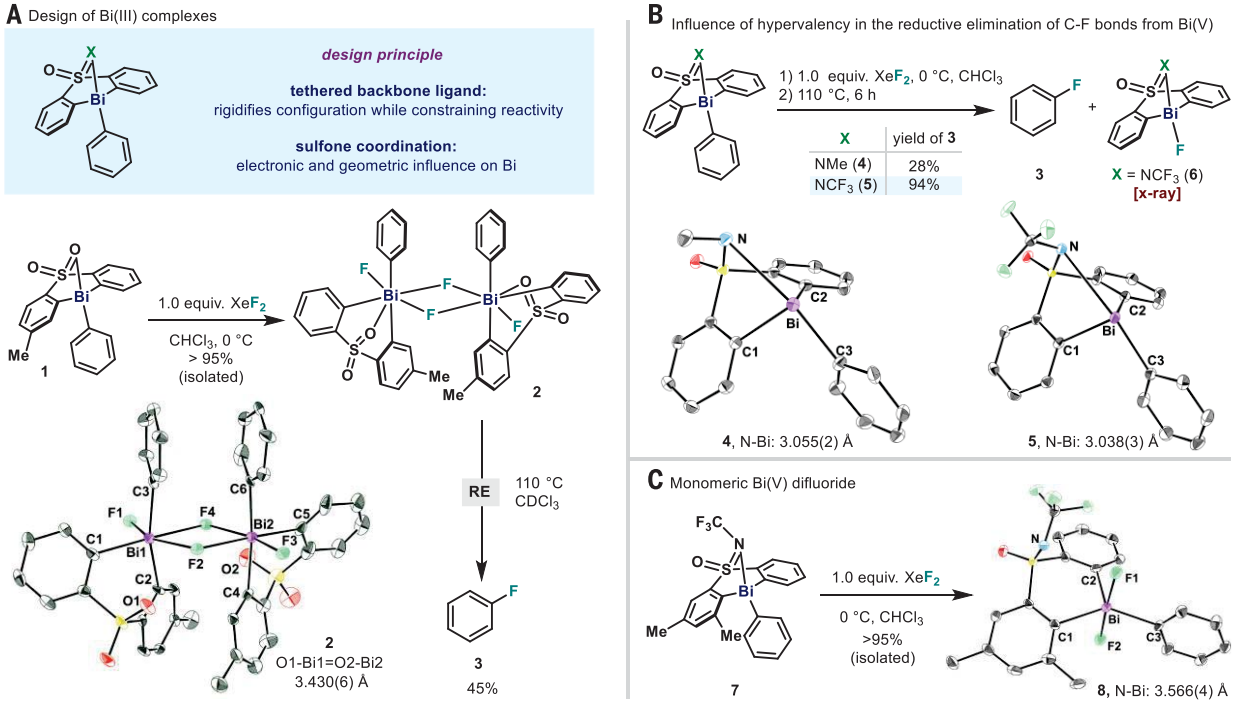

Fig. 2. Design principle and proof of concept. (**A**) Design of the bismine complexes to enable C–F reductive elimination. (**B**) Oxidative addition and reductive elimination sequence to forge C–F bonds. (**C**) Trigonal bipyramidal monomeric Bi(V) difluoride bearing NCF_3. Unless specified, yields were calculated by ^{19}F NMR.

and **6**, revealed a moderately positive slope (ρ = 0.43) when relative constants were plotted versus σ_p^+ (substituent constant), showing good linearity (R^2 = 0.9735, where R_2 is the coefficient of determination and R is the coefficient of correlation). This indicates a slightly faster reductive elimination when electron-withdrawing groups are present in the aryl ring (*39*, *45*). Furthermore, a slower reaction rate for the thermal decay of **14** at 90°C in $CDCl_3$ was obtained in the presence of 1.0 equivalent (equiv.) of Bu_4NF (Bu, butyl group) ($k_{obs} \approx 3.5 \times 10^{-5}$ s^{-1}, partial decomposition observed). Thus, the highly negative entropic value, the excellent linearity obtained when resonance effects are considered, and the slower rate in the presence of fluoride anions suggest a cationic intermediate **14-cation** (Fig. 3B) in equilibrium with **14** (*39*, *43*, *45*). From

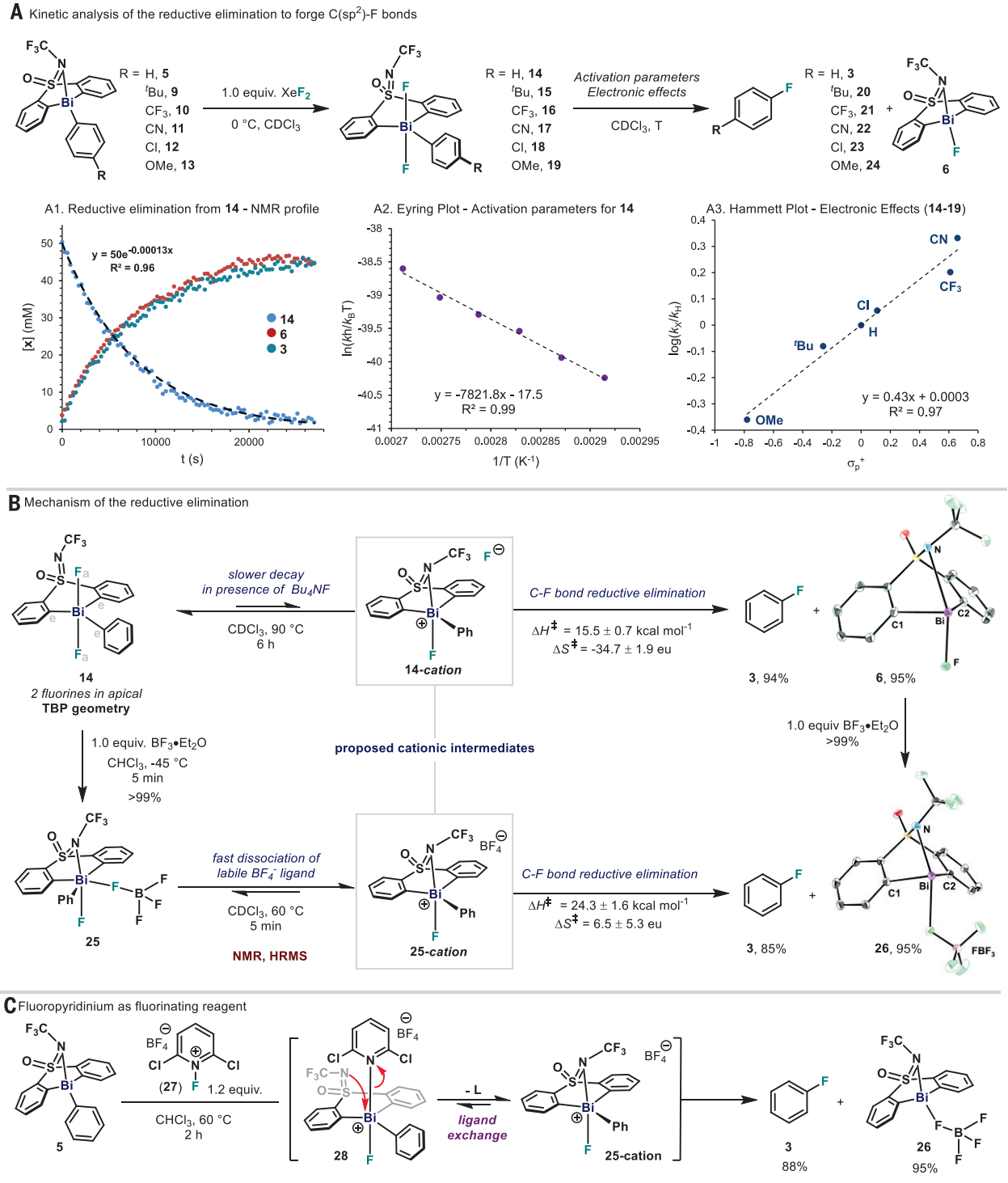

Fig. 3. Mechanistic studies of the reductive elimination. (**A**) Kinetic profile of the reductive elimination from **14**, Eyring analysis, and Hammett studies. (**B**) Experimental evaluation of the reductive elimination step. a, apical position; e, equatorial position. (**C**) Use of fluoropyridinium salts as fluorinating agents. h, hours; k, reaction rate constant; k_B, Boltzmann constant; T, temperature; k_X, reaction rate constant with para-substituent X; k_H, reaction rate constant with para-substituent H; eu, entropy unit.

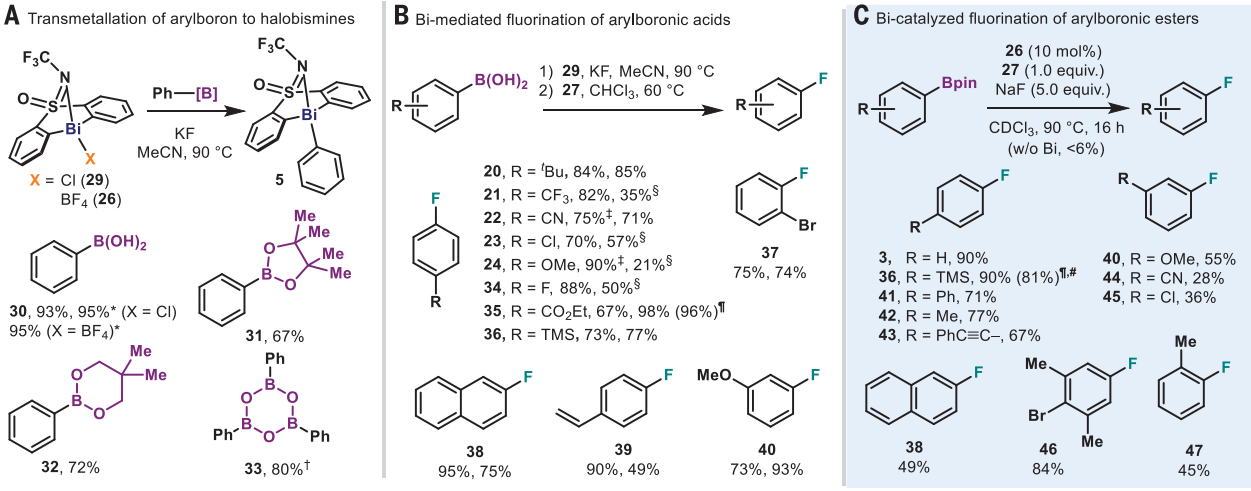

Fig. 4. Bi-mediated fluorination of organoboron compounds. (**A**) Transmetallation of boronic acid derivatives to a Bi(III) complex. Standard conditions: bismine (1.0 equiv.), arylboronic acid derivative (2.0 equiv.), KF (3.0 equiv.), CH_3CN, 90°C, 16 hours. (**B**) Two-step method for the fluorination of boronic acids. Yields are given for step 1 (isolated) and step 2 (determined by ^{19}F NMR), respectively. Step 1: chlorobismine **29** (1.0 equiv.), arylboronic acid (2.0 equiv.), KF (3.0 equiv.), CH_3CN, 90°C, 16 hours. Step 2: arylbismine (1.0 equiv.), **27** (1.1 equiv.), $CHCl_3$, 60°C, 6 hours. (**C**) Catalytic fluorination of aryl boronic esters. Standard conditions: **26** (10 mol%), **27** (1.0 equiv.), arylboronic pinacol ester (3.0 equiv.), NaF (5.0 equiv.), $CDCl_3$, 90°C, 16 hours. Yields determined by ^{19}F NMR. * denotes use of $CHCl_3$ as solvent. † denotes use of 0.66 equiv. of **33**. ‡ denotes use of K_2CO_3 as base. § denotes reaction performed at 110°C. ¶ denotes yield of isolated material after column chromatography. # denotes isolated product contains ~5% of proto-deborylated arene. ^{t}Bu, *tert*-butyl; TMS, trimethylsilyl.

this, elimination of fluorobenzene (**3**) is proposed, with concomitant formation of fluorobismine (**6**). In **14-cation**, coordination of the NCF_3 group to the Bi is expected, providing these Bi intermediates with the adequate balance between stabilization and electronic perturbation to enable C–F bond formation. Reductive elimination from pentavalent complexes with TBP geometry is usually governed by orbital symmetry rules; the Woodward-Hoffmann model (*46*–*48*) predicts that the coupling of equatorial-equatorial and apical-apical ligands should be much more favorable than the equatorial-apical coupling apparently observed in PhF (Ph, phenyl group) elimination from **14**. Recently, Paton and McNally have reported the possibility of bypassing these rules in pentavalent TBP P-based compounds via alternative mechanisms (*49*). Therefore, the formation of a cationic Bi intermediate represents another example which circumvents this constraint (*50*).

To assess the formation of cation intermediates experimentally, we speculated that a Lewis acid could coordinate the apical fluorine syn to the NCF_3 group in **14** and thereby notably elongate the Bi–F bond (*51*), leading to a compound that is geometrically similar to **14-cation**. When **14** was mixed with 1.0 equiv. of $BF_3{\cdot}OEt_2$ (Et, ethyl group) at –45°C (Fig. 3B), exclusive formation of **25** was confirmed in solution by ^1H, ^{11}B, ^{19}F, and ^{13}C nuclear magnetic resonance (NMR) and high-resolution mass spectrometry (HRMS). When this complex was heated to 60°C, fluorobenzene (**3**) was formed in just 5 min, with concomitant formation of tetrafluoroborate bismine (**26**). To further confirm the nature of **26**, 1.0 equiv. of $BF_3{\cdot}OEt_2$ was added to **6**, and immediate conversion to **26** (whose structure was confirmed by x-ray crystallography) was observed. In this case, because of the weakly coordinating nature of the tetrafluoroborate ligand, formation of **3** and **26** occurs readily from the cationic species **25-cation**. An Eyring analysis of the reductive elimination from in situ generated **25** (fig. S11) revealed a high enthalpic contribution to forge **3** and **26** ($\Delta H^{\ddagger}$ = 24.3 ± 1.6 kcal mol^{-1}). In contrast to complex **14**, the reductive elimination from this cationic intermediate showed a minimal entropic contribution ($\Delta S^{\ddagger}$ = 6.48 ± 5.3 e.u.) (*39*). Taken together, these results provide additional evidence for the intermediacy of a cationic species in the reductive elimination from the pentavalent difluorobismine **14**. With this mechanistic information in hand, we hypothesized that a milder and more synthetically useful fluorinating oxidant could afford similar intermediates. Oxidation of Bi(III) compounds to high-valent Bi(V) fluorides has been limited to strong fluorinating agents, such as XeF_2 or F_2 (*40*, *41*). However, when complex **5** was mixed with 1.2 equiv. of 1-fluoro-2,6-dichloropyridinium **27** in $CHCl_3$ (*52*), smooth C–F bond formation occurred at 60°C (Fig. 3C). The high conversion was ascribed to the high lability of the neutral and sterically encumbered 2,6-dichloropyridine ligand after oxidation (**28**), thus enabling coordination of the lone pair from the NCF_3 handle. The resulting intermediate (**25-cation**) can then eliminate fluorobenzene (**3**) and form the corresponding bismine (**26**).

With the goal of turning over the catalytic cycle, we then focused our attention on the transmetallation process between organoboron compounds and chlorobismines derived from **4** and **5** (**29** and **29-Me**) (Fig. 4A). Whitmire reported the possibility of transmetallating highly nucleophilic tetrarylborates with Bi salicylate salts (*53*). However, transmetallation of less-nucleophilic organoboron compounds to (pseudo)halobismines remains a challenge. Capitalizing on the use of KF as activator, when boronic acid (**30**) was mixed with **29**, smooth transmetallation took place (93% yield). When tetrafluoroborate bismine (**26**) was subjected to transmetallation, a 95% yield of **5** was obtained. Under the same conditions, other organoboron compounds such as PhBpin (pin, pinacol group) (**31**, 67%), PhB(neop) (neop, neopentyl glycolato group) (**32**, 72%), and $(PhBO)_3$ (**33**, 80%) were converted in good yields to phenylbismine (**5**), demonstrating versatility. With the aim of exploring the scope of a two-step method for fluorination, transmetallation of various phenylboronic acids was surveyed. High yields of arylation were obtained (67 to 90%), independently of the functional group in the aryl ring. The resulting arylbismines were then oxidized with **27** and reacted, as above, to release the corresponding arylfluorides (Fig. 4B). The protocol proved general with a variety of *para*-substituted arylfluorides including *tert*-butyl (**20**, 85%), trifluoromethyl (**21**, 35%), cyano (**22**, 71%), chloride (**23**, 57%), methoxy (**24**, 21%), fluoride (**34**, 50%), ester

(**35**, 96%), and trimethylsilyl (**36**, 77%) substituents. Furthermore, *ortho*-bromide (**37**, 74%), naphthalene (**38**, 75%), vinyl (**39**, 49%), and *meta*-methoxy (**40**, 93%) groups could also be accommodated.

We then turned our attention to merging all these steps into a catalytic cycle. On the basis of our initial hypothesis (Fig. 1B), transmetallation of an arylboronic acid derivative to an electrophilic Bi(III) center (**I**) would deliver the aryl bismine (**II**). Subsequently, **II** could be oxidized by the electrophilic fluorine source **27** to furnish a high-valent Bi(V) compound containing both fluoride and tetrafluoroborate ligands (**III**). Rapid decomposition of this intermediate would forge a C–F bond and **I**, thereby restoring the catalyst. Indeed, using tetrafluoroborate bismine (**26**), a catalytic protocol based on Bi for the oxidative fluorination of arylboronic esters was successfully implemented. After a short optimization of the fluoride source, required to activate the boronic ester, a variety of ArBpin were smoothly converted to the corresponding aryl fluorides (Fig. 4C). Using 10 mole % of bismine (**26**), phenylboronic acid pinacol ester (**31**) afforded a 90% yield of fluorobenzene (**3**). Substitution in *para*-position was also tolerated, as exemplified by the presence of trimethylsilyl (**36**, 90%), phenyl (**41**, 71%), methyl (**42**, 77%), alkynyl (**43**, 67%), and bromo (**46**, 84%) groups. Substitution of the aryl group at the *meta*-position presented more difficulties, affording moderate yields of aryl fluoride: methoxy (**40**, 55%), cyano (**44**, 28%), and chloride (**45**, 36%). π-Extended aromatics (**38**, 49%) and sterically hindered substitution, such as a Me group at the ortho position (**47**, 45%), were also amenable for fluorination. The Bi catalyst was essential for the reaction to proceed.

The design presented here enables a Bi complex to undergo transmetallation, oxidative addition with a mild fluorinating agent, and C–F reductive elimination to deliver aryl fluoride compounds. A detailed study of each step paved the way to the development of a catalytic cycle based on the Bi(III)/Bi(V) redox couple, a feat that remained elusive for Bi until now. This mode of reactivity for Bi represents a step forward in mimicking transition-metal–like behavior by an element outside the *d*-block. Although still limited to considerably oxidizing electrophiles and narrow substrate scope, the possibility of performing redox processes with Bi complexes by careful tuning of the ligand properties could potentially be expanded to other similar scenarios, in which a catalyst maneuvers between different oxidation states—a property traditionally associated with transition metals.

REFERENCES AND NOTES

1. A. de Meijere, F. Diederich, Eds., *Metal-Catalyzed Cross-Coupling Reactions* (Wiley, 2004).
2. J. E. Zweig, D. E. Kim, T. R. Newhouse, *Chem. Rev.* **117**, 11680–11752 (2017).
3. B. Su, Z.-C. Cao, Z.-J. Shi, *Acc. Chem. Res.* **48**, 886–896 (2015).
4. R. J. M. Klein Gebbink, M. Moret, Eds., *Non-Noble Metal Catalysis: Molecular Approaches and Reactions* (Wiley, 2019).
5. R. L. Melen, *Science* **363**, 479–484 (2019).
6. P. P. Power, *Nature* **463**, 171–177 (2010).
7. C. Weetman, S. Inoue, *ChemCatChem* **10**, 4213–4228 (2018).
8. G. C. Welch, R. R. San Juan, J. D. Masuda, D. W. Stephan, *Science* **314**, 1124–1126 (2006).
9. L. Wu *et al*., *Nat. Commun.* **10**, 2786 (2019).
10. A. A. Toutov *et al*., *Nature* **518**, 80–84 (2015).
11. H. Bauer *et al*., *Nat. Catal.* **1**, 40–47 (2018).
12. M.-A. Légaré, M.-A. Courtemanche, É. Rochette, F.-G. Fontaine, *Science* **349**, 513–516 (2015).
13. I. G. Molnár, R. Gilmour, *J. Am. Chem. Soc.* **138**, 5004–5007 (2016).
14. N. L. Dunn, M. Ha, A. T. Radosevich, *J. Am. Chem. Soc.* **134**, 11330–11333 (2012).
15. J. C. Sarie, J. Neufeld, C. G. Daniliuc, R. Gilmour, *ACS Catal.* **9**, 7232–7237 (2019).
16. S. M. Banik, J. W. Medley, E. N. Jacobsen, *J. Am. Chem. Soc.* **138**, 5000–5003 (2016).
17. T. V. Nykaza *et al*., *J. Am. Chem. Soc.* **140**, 15200–15205 (2018).
18. R. Mohan, *Nat. Chem.* **2**, 336 (2010).
19. M. B. Kindervater, K. M. Marczenko, U. Werner-Zwanziger, S. S. Chitnis, *Angew. Chem. Int. Ed.* **58**, 7850–7855 (2019).
20. T. Ollevier, Ed., *Bismuth-Mediated Organic Reactions* (Springer, 2012).
21. B. Ritschel, J. Poater, H. Dengel, F. M. Bickelhaupt, C. Lichtenberg, *Angew. Chem. Int. Ed.* **57**, 3825–3829 (2018).
22. J. Ramler *et al*., *Chem. Sci.* **10**, 4169–4176 (2019).
23. F. Wang, O. Planas, J. Cornella, *J. Am. Chem. Soc.* **141**, 4235–4240 (2019).
24. J. Ramler, I. Krummenacher, C. Lichtenberg, *Angew. Chem. Int. Ed.* **58**, 12924–12929 (2019).
25. R. J. Schwamm, M. Lein, M. P. Coles, C. M. Fitchett, *Chem. Commun.* **54**, 916–919 (2018).
26. S. Yamago *et al*., *Angew. Chem. Int. Ed.* **46**, 1304–1306 (2007).
27. G. Pattison, *Org. Biomol. Chem.* **17**, 5651–5660 (2019).
28. P. S. Fier, J. Luo, J. F. Hartwig, *J. Am. Chem. Soc.* **135**, 2552–2559 (2013).
29. M. Tredwell *et al*., *Angew. Chem. Int. Ed.* **53**, 7751–7755 (2014).
30. Y. Ye, M. S. Sanford, *J. Am. Chem. Soc.* **135**, 4648–4651 (2013).
31. T. Furuya, H. M. Kaiser, T. Ritter, *Angew. Chem. Int. Ed.* **47**, 5993–5996 (2008).
32. T. Furuya, T. Ritter, *Org. Lett.* **11**, 2860–2863 (2009).
33. B. H. Rotstein, N. A. Stephenson, N. Vasdev, S. H. Liang, *Nat. Commun.* **5**, 4365 (2014).
34. A. R. Mazzotti, M. G. Campbell, P. Tang, J. M. Murphy, T. Ritter, *J. Am. Chem. Soc.* **135**, 14012–14015 (2013).
35. J.-P. Finet, Ed., *Ligand Coupling Reactions with Heteroatomic Compounds* (Elsevier, 1998).
36. G. G. Briand, N. Burford, *Adv. Inorg. Chem.* **50**, 285–357 (2000).
37. K. Ohkata, S. Takemoto, M. Ohnishi, K.-Y. Akiba, *Tetrahedron Lett.* **30**, 4841–4844 (1989).
38. I. Ugi, D. Marquarding, H. Klusacek, P. Gillespie, F. Ramirez, *Acc. Chem. Res.* **4**, 288–296 (1971).
39. T. Furuya *et al*., *J. Am. Chem. Soc.* **132**, 3793–3807 (2010).
40. T. Ooi, R. Goto, K. Maruoka, *J. Am. Chem. Soc.* **125**, 10494–10495 (2003).
41. S. A. Lermontov, I. M. Rakov, N. S. Zefirov, P. J. Stang, *Tetrahedron Lett.* **37**, 4051–4054 (1996).
42. E. L. Muetterties, W. Mahler, R. Schmutzler, *Inorg. Chem.* **2**, 613–618 (1963).
43. N. P. Mankad, F. D. Toste, *Chem. Sci.* **3**, 72–76 (2012).
44. A. J. Canty, H. Jin, B. W. Skelton, A. H. White, *Inorg. Chem.* **37**, 3975–3981 (1998).
45. J. M. Racowski, A. R. Dick, M. S. Sanford, *J. Am. Chem. Soc.* **131**, 10974–10983 (2009).
46. R. Hoffmann, J. M. Howell, E. L. Muetterties, *J. Am. Chem. Soc.* **94**, 3047–3058 (1972).
47. R. B. Woodward, R. Hoffmann, *Angew. Chem. Int. Ed.* **8**, 781–853 (1969).
48. K.-Y. Akiba, Ed., *Organo Main Group Chemistry* (Wiley, 2011).
49. M. C. Hilton *et al*., *Science* **362**, 799–804 (2018).
50. J. Moc, K. Morokuma, *J. Am. Chem. Soc.* **117**, 11790–11797 (1995).
51. Y. Matano, S. A. Begum, T. Miyamatsu, H. Suzuki, *Organometallics* **17**, 4332–4334 (1998).
52. G. S. Lal, G. P. Pez, R. G. Syvret, *Chem. Rev.* **96**, 1737–1756 (1996).
53. V. Stavila, J. H. Thurston, D. Prieto-Centurión, K. H. Whitmire, *Organometallics* **26**, 6864–6866 (2007).

ACKNOWLEDGMENTS

We thank A. Fürstner and T. Ritter for insightful discussions and generous support and B. Morandi and C. Obradors for insightful suggestions and for proofreading the manuscript. N. Noethling and R. Goddard are acknowledged for crystallographic data analysis. We also thank the analytical department at the MPI-Kohlenforschung for support in the characterization of compounds. **Funding:** Financial support for this work was provided by Max-Planck-Gesellschaft, Max-Planck-Institut für Kohlenforschung, Fonds der Chemischen Industrie (FCI-VCI), Alexander von Humboldt Foundation (to O.P.), and the European Commission (Marie Skłodowska Curie Fellowship, grant no. 833361, to O.P.). **Author contributions:** J.C. and O.P. conceived the idea. All experiments were conducted by O.P. and F.W. NMR experiments and analysis were conducted by O.P. and M.L. The manuscript was written by O.P. and J.C. The project was directed by J.C. **Competing interests:** The authors declare no competing interests. **Data and materials availability:** Crystallographic data for structures **2**, **4**, **5**, **6**, **7**, **8**, **26**, **29**, and **29-Me** are available free of charge from the Cambridge Crystallographic Data Center under reference numbers 1949430, 1949432, 1949433, 1949435, 1949434, 1949431, 1956313, 1949436, and 1980915, respectively.

SUPPLEMENTARY MATERIALS

science.sciencemag.org/content/367/6475/313/suppl/DC1
Materials and Methods
Figs. S1 to S27
Tables S1 to S23
Spectral Data
References (*54*–*69*)

26 August 2019; accepted 17 December 2019
10.1126/science.aaz2258